Asymmetric isolated skyrmions in polar magnets with easy-plane anisotropy

A. O. Leonov, István Kézsmárki

Angaben zur Veröffentlichung / Publication details:

Leonov, A. O., and István Kézsmárki. 2017. "Asymmetric isolated skyrmions in polar magnets with easy-plane anisotropy." *Physical Review B* 96 (1): 014423. https://doi.org/10.1103/physrevb.96.014423.

Asymmetric isolated skyrmions in polar magnets with easy-plane anisotropy

A. O. Leonov[1,2,*] and I. Kézsmárki[3,4]

[1]*Center for Chiral Science, Hiroshima University, Higashi-Hiroshima, Hiroshima 739-8526, Japan*
[2]*Department of Chemistry, Faculty of Science, Hiroshima University Kagamiyama, Higashi Hiroshima, Hiroshima 739-8526, Japan*
[3]*Experimental Physics V, Center for Electronic Correlations and Magnetism, University of Augsburg, Augsburg 86135, Germany*
[4]*Department of Physics, Budapest University of Technology and Economics and MTA-BME Lendület Magneto-Optical Spectroscopy Research Group, Budapest 1111, Hungary*

(Received 30 March 2017; published 17 July 2017)

We introduce a class of isolated magnetic skyrmions emerging within tilted ferromagnetic phases of polar magnets with easy-plane anisotropy. The asymmetric magnetic structure of these skyrmions is associated with an intricate pattern of the energy density, which exhibits positive and negative asymptotics with respect to the surrounding state with a ferromagnetic moment tilted away from the polar axis. Correspondingly, the skyrmion-skyrmion interaction has an anisotropic character and can be either attractive or repulsive depending on the relative orientation of the skyrmion pair. We investigate the stability of these asymmetric skyrmions against the elliptical cone state and follow their transformation into axisymmetric skyrmions, when the tilted ferromagnetic moment of the host phase is reduced. Our theory gives clear directions for experimental studies of isolated asymmetric skyrmions and their clusters embedded in tilted ferromagnetic phases.

DOI: 10.1103/PhysRevB.96.014423

I. INTRODUCTION

Magnetic chiral skyrmions are particlelike topological solitons with complex spin structure [1–4] which are the solutions of the field equations of the Dzyaloshinskii's theory [5]. Recently, skyrmion lattice states and isolated skyrmions were discovered in bulk crystals of chiral magnets near the magnetic ordering temperatures [6–8] and in nanostructures with confined geometries over larger temperature regions [9–12]. The small size, topological protection, and easy manipulation of skyrmions by electric fields and currents [13–15] generated enormous interest in their applications in information storage and processing [16,17]. Depending on the crystal symmetry of the host materials, distinct classes of skyrmions, such as Bloch and Néel skyrmions, or antiskyrmions [18] can be realized. In particular, Néel skyrmions were recently found in GaV_4S_8 and GaV_4Se_8, which are magnetic semiconductors with nonchiral but polar crystal structure [8,19]. Néel skyrmions emerging in such multiferroic hosts are associated with an electric polarization pattern, which can be exploited for their electric field control [20].

The current interest of skyrmionics is focused on isolated *axisymmetric* skyrmions within the polarized ferromagnetic (PFM) state of noncentrosymmetric magnets. All the spins around such skyrmions are parallel to the applied magnetic field and point opposite to the spin in the center of the skyrmion, as visualized in Figs. 1(a) and 1(c). The internal structure of such axisymmetric skyrmions, generally characterized by repulsive skyrmion-skyrmion interaction, has been thoroughly investigated theoretically [21,22] and experimentally by spin-polarized scanning tunneling microscopy in PdFe bilayers with surface-induced Dzyaloshinskii-Moriya interactions (DMIs) and strong easy-axis anisotropy [23,24]. The existence region of axisymmetric skyrmions was found to be restricted by strip-out instabilities at low fields and a collapse at high fields [22].

The internal spin pattern of isolated skyrmions can break the rotational symmetry once placed into the conical phase of bulk helimagnets [25], such as the cubic B20 compounds. These skyrmions are not uniform along their axes. Although their central core region nearly preserves the axial symmetry, the domain-wall region, which connects the core with the embedding conical state, is *asymmetric* [25]. This asymmetric profile of the cross section forms a screwlike modulation along the skyrmion core, as depicted in Figs. 1(b) and 1(d). These asymmetric isolated skyrmions, which can exhibit an *attractive* skyrmion-skyrmion interaction, were proposed to underlie the precursor phenomena near the ordering temperatures in chiral B20 magnets (MnSi, FeGe) [25] and have prospects in spintronics as an alternative to the common axisymmetric skyrmions [26].

In this paper we introduce a type of isolated skyrmions within the tilted ferromagnetic (TFM) state of magnets with polar crystal structure and easy-plane anisotropy. Such skyrmions are forced to develop an asymmetric shape in order to match their spin pattern with that of the TFM state, meanwhile preserving their topological charge $q = 1$. We find that—unlike the repulsive axisymmetric skyrmions and the attractive asymmetric skyrmions respectively embedded in the PFM state and the conical phase of chiral magnets—the asymmetric skyrmions emerging in the TFM state of polar magnets exhibit anisotropic interskyrmion potential. Depending on the relative orientation of the two individual skyrmions, this potential can be attractive, leading to the formation of biskyrmion or multiskyrmion states, or repulsive.

II. THE MODEL

Chiral solitons and modulated phases can be derived by minimizing the energy functional of a noncentrosymmetric ferromagnet [5,27,28]:

$$w = \sum_{i,j} (\partial_i m_j)^2 - k_u m_z^2 - \mathbf{m} \cdot \mathbf{h} + w_D. \qquad (1)$$

*leonov@hiroshima-u.ac.jp

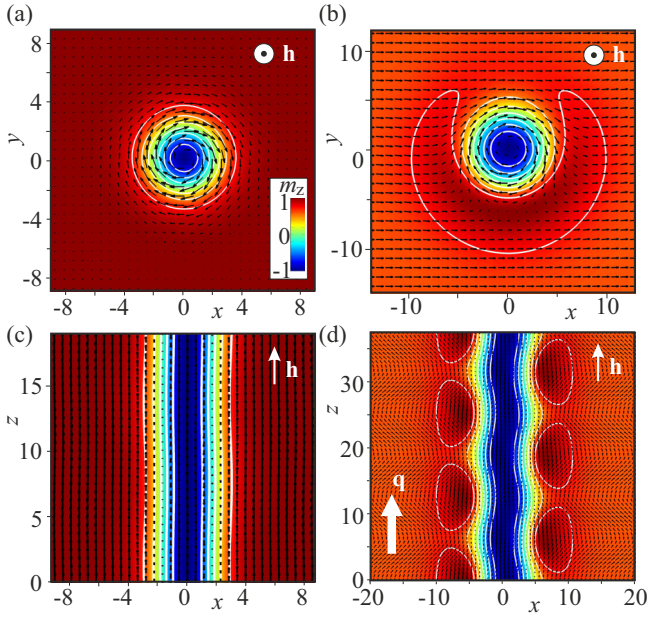

FIG. 1. Cross sections of the internal magnetic structures of skyrmions obtained in model (1) with DMI (2) and no axial anisotropy, $k_u = 0$. The magnetic field $\mathbf{h}$ is directed along the z axis. (a) and (c) Color plots of m_z for an axisymmetric skyrmion embedded within the PFM state ($h = 0.55$) in the xy and xz planes, respectively. (b) and (d) The same for a nonaxisymmetric skyrmion in the conical phase ($h = 0.3$), with an additional screwlike rotation alongside with the conical phase (white arrow shows the modulation vector $\mathbf{q}$ of the conical phase). The color bar in panel (a) is common for each panel. The in-plane component of the magnetization is represented by black arrows.

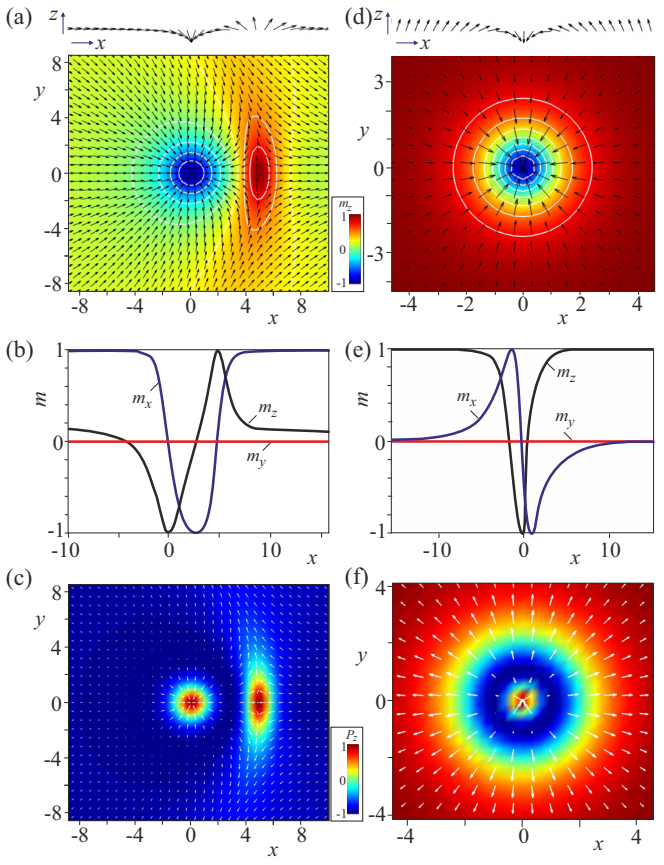

FIG. 2. Numerical solutions for skyrmions using model (1) with DMI (3). (a)–(c) Asymmetric skyrmions within the TFM state for $h = 0.5$ and $k_u = -1.1$. (d)–(f) Axisymmetric skyrmions within the PFM state for $h = 1.6$ and $k_u = -0.7$. The top panels are color plots of m_z in the xy plane with black arrows representing the in-plane magnetization components. The top insets show the magnetization components in the plane xz across the skyrmion centers, which are additionally shown as curves in the middle panels. Note that the m_x and m_z components seemingly exchange roles in panels (b) and (e), which is due to the different embedding phase, the TFM state with nearly in-plane magnetization, and the PFM state with fully out-of-plane magnetization. The bottom panels are color plots of P_z with white arrows representing the in-plane components of the electric polarization, calculated according to Eq. (6).

Here, we use reduced values of the spatial variable, $\mathbf{x} = \mathbf{r}/L_D$ with $L_D = A/D$ being the periodicity of the modulated states. A is the exchange stiffness constant. The sign of the Dzyaloshinskii constant D determines the sense of rotation. $k_u = K_u A/D^2 < 0$ is the uniaxial anisotropy of easy-plane type, $\mathbf{m} = [\sin\theta\ \cos\psi, \sin\theta\ \sin\psi, \cos\theta]$ is the unity vector along the magnetization, and $\mathbf{h} = \mathbf{H}A/D^2$ is the applied magnetic field in reduced units.

Depending on the crystal symmetry, the DMI energy w_D includes certain combinations of Lifshitz invariants $\mathcal{L}^{(k)}_{i,j} = m_i \partial m_j/\partial x_k - m_j \partial m_i/\partial x_k$ [2,5]. Particularly, for cubic helimagnets, such as MnSi [6], FeGe [10], Cu_2OSeO_3 [29], and β-type Mn alloys [30], belonging to the chiral 23 (T) and 432 (O) crystallographic classes, the DMI is reduced to the following form:

$$w_D = \mathbf{m} \cdot (\nabla \times \mathbf{m}) \tag{2}$$

and stabilizes Bloch-type modulations. Two types of isolated skyrmions have been found to exist for DMI (2): axisymmetric skyrmions within the PFM state and asymmetric skyrmions within the conical phase, respectively visualized in Figs. 1(a) and 1(b).

In the phase diagram of noncentrosymmetric ferromagnets with DMI (2) and easy-plane uniaxial anisotropy, the conical phase is the only stable modulated state [31–33]. Other states including skyrmion lattices and spirals are only metastable solutions of the model, although they can be stabilized in real materials by several means, such as thermal fluctuations and confined geometry. Axisymmetric isolated skyrmions exist as metastable excitations of the PFM state for $h > 0.5 - 2k_u$, while asymmetric skyrmions are present for $h < 0.5 - 2k_u$ [31].

The form of DMI is different for materials belonging to polar uniaxial (C_{nv}) crystallographic classes,

$$w_D = m_x \partial_x m_z - m_z \partial_x m_x + m_y \partial_y m_z - m_z \partial_y m_y, \tag{3}$$

which are the subject of the present work. This type of DMI can stabilize skyrmions and spirals (cycloids) of Néel type with the rotation plane of the magnetization including the wave vector and the polar axis (Fig. 2). As the conical phase is suppressed in this case, the phase diagram reveals wide regions of different states with one- and two-dimensional modulations [33–35], as

discerned in Figs. 1 and 4 of the Supplemental Material [36]. The TFM and PFM states in polar magnets with easy-plane anisotropy host two distinct types of isolated skyrmions, as shown in Fig. 2.

III. THE PROPERTIES OF ISOLATED NÉEL SKYRMIONS

Isolated axisymmetric Néel skyrmions within the PFM phase are characterized by azimuthal (θ) and polar (ψ) angles of the spins according to

$$\theta = \theta(\rho), \quad \psi = \varphi. \tag{4}$$

Here the boundary conditions are $\theta(0) = \pi$, $\theta(\infty) = 0$, while φ and ρ are cylindrical coordinates of the spatial variable.

On the other hand, the isolated Néel skyrmions embedded in the TFM phase are confined by the following in-plane boundary conditions:

$$\theta(0) = \pi, \quad \theta(\infty) = \theta_{\mathrm{TFM}} = \arccos(h/2k_u). \tag{5}$$

These boundary conditions violate the rotational symmetry, forcing the skyrmions to develop an asymmetric shape.

A. Internal structure

The results of the numerical minimization of the energy functional (1) with boundary conditions (5) are shown in Figs. 2(a) and 2(b). When the canted moment of the TFM state is along the y axis, the asymmetry is clearly reflected in both m_x and m_z. As implied by m_z, such skyrmions consist of a strongly localized nearly axisymmetric core and an asymmetric transitional region toward the TFM state. From the left side of the depicted skyrmion, the magnetization rotates directly from θ_{TFM} to $\theta = \pi$ in the skyrmion center. In contrast, at the right side, the magnetization first passes through $\theta = 0$ ($m_z = 1$) and then converges back to θ_{TFM}. This is the reason for the crescent-shaped anti-skyrmion-like region with a positive energy density over the TFM state, shown in Figs. 3(b) and 3(c), which is necessary to maintain the topological charge $q = 1$ of such a highly distorted asymmetric skyrmion.

B. Polarization pattern

As already mentioned, Néel skyrmions in insulating hosts can have a polar dressing in addition to their magnetic pattern. The asymmetry of Néel skyrmions embedded in the TFM phase is also reflected in the spatial pattern of their electric polarization, as visualized in Fig. 2(c) in comparison with the polar pattern of an axisymmetric Néel skyrmion in Fig. 2(f). The magnetically induced polarization was calculated using the lowest-order magnetoelectric terms allowed in materials with C_{4v} or C_{6v} symmetry:

$$\mathbf{P} = \left[\alpha m_x m_z, \alpha m_y m_z, \beta m_z^2 + \gamma\left(m_x^2 + m_y^2\right)\right]. \tag{6}$$

For the polarization patterns shown in Figs. 2(c) and 2(f), we set $\alpha = \beta = -\gamma$ and used the normalization condition, $|\mathbf{m}| = 1$. While the feasibility of electric-field-driven switching has been demonstrated already for Néel skyrmions [15], the asymmetry of the polarization pattern, characteristic to the isolated skyrmions studied here, can be exploited to control their orientation by in-plane electric fields.

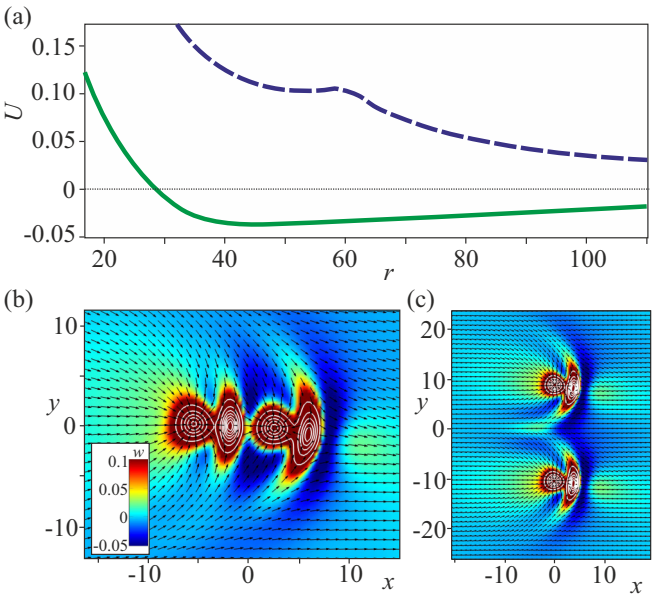

FIG. 3. (a) The interskyrmion potential U versus the distance r between the skyrmion centers. $U(r)$ was calculated by imposing the constraint, $m_z = -1$, at the skyrmion centers [28] and minimizing the energy with respect to spins at all other sites ($h = 0.5$, $k_u = -1.1$). Contour plots of the energy density distribution $w(x, y)$ for (b) a bound pair of asymmetric skyrmions in the head-to-head configuration and (c) a repulsive pair of asymmetric skyrmions in the side-by-side configuration. Black arrows represent the in-plane magnetization components. The energy scale, common for panels (b) and (c), is chosen in the range $(-0.05, 0.1)$ to highlight the interskyrmion regions.

C. Skyrmion-skyrmion interaction

Asymmetric skyrmions within the TFM phase can be considered as xy cross sections of asymmetric skyrmions in the conical phases, shown in Figs. 1(b) and 1(d) [25,26]. However, the DMI term (3) stabilizing Néel skyrmions does not support any modulation along the z axis. Thus, the asymmetry of Néel skyrmions created within the TFM state is uniform along the z axis, which results in a nontrivial character of interskyrmion potential, displayed in Fig. 3(a). Figures 3(b) and 3(c) present energy density distributions in skyrmion pairs for two mutual orientations, head-to-head and side-by-side. In the head-to-head configuration, skyrmions form pairs with a fixed interskyrmion distance, implying the attractive nature of their interaction, as clear from the green curve in Fig. 3(a). Therefore, these skyrmions are expected to form one-dimensional chains running along the canted magnetization component of the TFM phase [37]. The calculated interskyrmion potential for the side-by-side configuration, the blue curve in Fig. 3(a), reveals the repulsive character of skyrmion-skyrmion interaction at large distances with a local minimum (or saddle point) at smaller distances. Such a behavior of the interskyrmion potential is related to the positive and negative asymptotics of the energy density toward the TFM state. In general, we argue that the interskyrmion potential inherently contains a number of minima separated by saddle points (see also the Supplemental Material [36] and Ref. [38] for additional details).

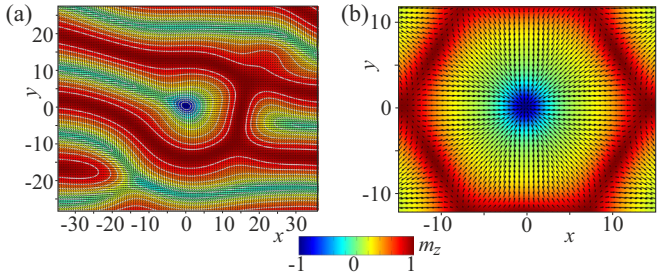

FIG. 4. (a) Instability of an isolated Néel skyrmion with respect to the elliptical cone state as obtained for $h = 0.5$ and $k_u = -0.5$. (b) The structure of skyrmions in the hexagonal skyrmion lattice for $h = 0.5$ and $k_u = -0.7$.

In contrast, the asymmetric pattern of Bloch skyrmions is tightly linked to the conical modulation of the host phase and rotates around the z axis in the same way for each individual skyrmion. This synchronized screwlike rotation of the asymmetry for a pair of such skyrmions leads to an overall attractive potential, by averaging over head-to-head, side-by-side, and intermediate configurations alternating along the z axis [25].

D. Elliptical instability

The asymmetric skyrmions within the TFM state can exist only for $k_u < -1$, i.e., require a relatively strong easy-plane anisotropy. For $k_u > -1$ isolated skyrmions undergo an instability toward the elliptical cone state, as demonstrated in Fig. 4(a) (see Ref. [33] and the Supplemental Material [36] for detailed information on the structure of the elliptical cone and its lability region). This instability resembles the elliptical instability of skyrmions into spirals considered in Ref. [22] and allows one to generalize the considered phenomenon: isolated skyrmions tend to elongate into one-dimensional states (elliptical cones or spirals) which have smaller energy for given control parameters.

The TFM state turns into the PFM state with $\theta_{\mathrm{PFM}} = 0$ at the line $h = 2k_u$. In the PFM state the rotational symmetry is recovered and isolated skyrmions become axisymmetric with $\theta = \theta(\rho)$ and $\psi = \phi$, as shown in Figs. 2(d) and 2(e). The core region and the surrounding ring have positive and negative energy densities, respectively, implying a repulsive skyrmion-skyrmion interaction [1].

Néel skyrmions can also form the thermodynamically stable skyrmion lattices. Skyrmions within unit cells of such lattices have perfectly hexagonal shape, as seen in Fig. 4(b), and do not bear any hint on the asymmetric skyrmion structure or skyrmion instability into the elliptical cone.

Results obtained within the model (1) with DMI (3) are valid for *bulk* polar magnets with axial symmetry as well as for *thin films* with interface-induced DMI. In particular, bulk polar magnetic semiconductors GaV_4S_8 [8] and GaV_4Se_8 [19] with the C_{3v} symmetry possess uniaxial anisotropy of easy-axis and easy-plane type, respectively. Since the magnitude of the effective anisotropy in these lacunar spinels strongly varies with temperature, this material family provides an ideal arena for the comprehensive study of anisotropic effects on modulated magnetic states [19]. Skyrmions were also studied experimentally in various systems with interface-induced DMI [23,24,39,40]. In these thin-film structures, the rotational symmetry can also be broken by different anisotropic environments due to lattice strains or reconstructions in the magnetic surface layers [41], as has been discussed recently for the double atomic layers of Fe on Ir(111) [42]. These structural anisotropies also promote the formation of asymmetric skyrmions.

IV. CONCLUSIONS

In conclusion, we found a type of isolated skyrmions emerging in tilted ferromagnetic (FM) states of polar magnets with easy-plane anisotropy. These solitonic states are characterized by an asymmetric shape and an anisotropic interskyrmion potential. Our results are of particular interest for two-dimensional materials like thin films, surfaces, and interfaces, where easy-plane anisotropy can coexist with Rashba-type spin-orbit coupling, activated by the broken surface-inversion symmetry [33,35]. In order to fully explore their characteristics and functionalities, the internal structure of these asymmetric skyrmions should be studied experimentally, as was done for the axisymmetric individual skyrmions within polarized FM states [23,24].

ACKNOWLEDGMENTS

The authors are grateful to K. Inoue, A. Bogdanov, and Y. Togawa for useful discussions. This work was funded by JSPS Core-to-Core Program, Advanced Research Networks (Japan). This work was supported by the Hungarian Research Fund OTKA K 108918.

[1] A. Bogdanov and A. Hubert, J. Magn. Magn. Mater. **138**, 255 (1994); **195**, 182 (1999).
[2] A. N. Bogdanov and D. A. Yablonskii, Zh. Eksp. Teor. Fiz. **95**, 178 (1989) [Sov. Phys. JETP **68**, 101 (1989)].
[3] N. Nagaosa and Y. Tokura, Nat. Nanotechnol. **8**, 899 (2013).
[4] U. K. Rößler, A. A. Leonov, and A. N. Bogdanov, J. Phys.: Conf. Ser. **303**, 012105 (2011).
[5] I. E. Dzyaloshinskii, Zh. Eksp. Teor. Fiz. **46**, 1420 (1964) [Sov. Phys. JETP **19**, 960 (1964)].
[6] S. Mühlbauer, B. Binz, F. Jonietz, C. Pfleiderer, A. Rosch, A. Neubauer, R. Georgii, and P. Böni, Science **323**, 915 (2009).
[7] H. Wilhelm, M. Baenitz, M. Schmidt, U. K. Rößler, A. A. Leonov, and A. N. Bogdanov, Phys. Rev. Lett. **107**, 127203 (2011).
[8] I. Kezsmarki *et al.*, Nat. Mater. **14**, 1116 (2015).
[9] X. Z. Yu, Y. Onose, N. Kanazawa, J. H. Park, J. H. Han, Y. Matsui, N. Nagaosa, and Y. Tokura, Nature (London) **465**, 901 (2010).

[10] X. Z. Yu, N. Kanazawa, Y. Onose, K. Kimoto, W. Z. Zhang, S. Ishiwata, Y. Matsui, and Y. Tokura, Nat. Mater. **10**, 106 (2011).
[11] H. Du *et al.*, Nat. Commun. **6**, 7637 (2015).
[12] D. Liang, J. P. DeGrave, M. J. Stolt, Y. Tokura, and S. Jin, Nat. Commun. **6**, 8217 (2015).
[13] T. Schulz, R. Ritz, A. Bauer, M. Halder, M. Wagner, C. Franz, C. Pfleiderer, K. Everschor, M. Garst, and A. Rosch, Nat. Phys. **8**, 301 (2012).
[14] F. Jonietz, S. Mühlbauer, C. Pfleiderer, A. Neubauer, W. Mnzer, A. Bauer, T. Adams, R. Georgii, P. Böni, R. A. Duine, K. Everschor, M. Garst, and A. Rosch, Science **330**, 1648 (2010).
[15] P.-J. Hsu, A. Kubetzka, A. Finco, N. Romming, K. von Bergmann, and R. Wiesendanger, Nat. Nanotechnol. **12**, 123 (2016).
[16] J. Sampaio, V. Cros, S. Rohart, A. Thiaville, and A. Fert, Nat. Nanotechnol. **8**, 839 (2013).
[17] E. M. R. Tomasello, R. Zivieri, L. Torres, M. Carpentieri, and G. Finocchio, Sci. Rep. **4**, 6784 (2014).
[18] A. K. Nayak, V. Kumar, P. Werner, E. Pippel, R. Sahoo, F. Damay, U. K. Rößler, C. Felser, and S. S. P. Parkin, arXiv:1703.01017.
[19] S. Bordács *et al.* [Sci. Rep. (to be published)].
[20] E. Ruff, S. Widmann, P. Lunkenheimer, V. Tsurkan, S. Bordács, I. Kézsmárki, and A. Loidl, Sci. Adv. **1**, e1500916 (2015).
[21] A. Bogdanov and A. Hubert, Phys. Status Solidi B **186**, 527 (1994).
[22] A. O. Leonov, T. L. Monchesky, N. Romming, A. Kubetzka, A. N. Bogdanov, and R. Wiesendanger, New J. Phys. **18**, 065003 (2016).
[23] N. Romming, C. Hanneken, M. Menzel, J. E. Bickel, B. Wolter, K. von Bergmann, A. Kubetzka, and R. Wiesendanger, Science **341**, 636 (2013).
[24] N. Romming, A. Kubetzka, C. Hanneken, K. von Bergmann, and R. Wiesendanger, Phys. Rev. Lett. **114**, 177203 (2015).
[25] A. O. Leonov, T. L. Monchesky, J. C. Loudon, and A. N. Bogdanov, J. Phys.: Condens. Matter **28**, 35LT01 (2016).
[26] A. O. Leonov, J. C. Loudon, and A. N. Bogdanov, Appl. Phys. Lett. **109**, 172404 (2016).
[27] P. Bak and M. H. Jensen, J. Phys. C: Solid State Phys. **13**, L881 (1980); O. Nakanishi, A. Yanase, A. Hasegawa, and M. Kataoka, Solid State Commun. **35**, 995 (1980).
[28] A. A. Leonov, Ph.D. thesis, Technical University Dresden, 2012.
[29] S. Seki, X. Z. Yu, S. Ishiwata, and Y. Tokura, Science **336**, 198 (2012).
[30] Y. Tokunaga, X. Z. Yu, J. S. White, H. M. Rønnow, D. Morikawa, Y. Taguchi, and Y. Tokura, Nat. Commun. **6**, 7638 (2015).
[31] M. N. Wilson, A. B. Butenko, A. N. Bogdanov, and T. L. Monchesky, Phys. Rev. B **89**, 094411 (2014).
[32] A. B. Butenko, A. A. Leonov, U. K. Rößler, and A. N. Bogdanov, Phys. Rev. B **82**, 052403 (2010).
[33] J. Rowland, S. Banerjee, and M. Randeria, Phys. Rev. B **93**, 020404 (2016).
[34] U. Güngördü, R. Nepal, O. A. Tretiakov, K. Belashchenko, and A. A. Kovalev, Phys. Rev. B **93**, 064428 (2016).
[35] S. Banerjee, J. Rowland, O. Erten, and M. Randeria, Phys. Rev. X **4**, 031045 (2014).
[36] See Supplemental Material at http://link.aps.org/supplemental/10.1103/PhysRevB.96.014423 for details on the elliptical cone structure and the phase diagrams of states.
[37] S.-Z. Lin, A. Saxena, and C. D. Batista, Phys. Rev. B **91**, 224407 (2015).
[38] A. O. Leonov and M. Mostovoy, Nat. Commun. **6**, 8275 (2015).
[39] B. Dúpe, G. Bihlmayer, M. Böttcher, S. Blügel, and S. Heinze, Nat. Commun. **7**, 11779 (2016).
[40] S. Woo, K. Litzius, B. Krüger, M. Im, L. Caretta, K. Richter, M. Mann, A. Krone, R. Reeve, M. Weigand *et al.*, Nat. Mater. **15**, 501 (2016).
[41] J. Hagemeister, E. Y. Vedmedenko, and R. Wiesendanger, Phys. Rev. B **94**, 104434 (2016).
[42] P. J. Hsu, A. Finco, L. Schmidt, A. Kubetzka, K. von Bergmann, and R. Wiesendanger, Phys. Rev. Lett. **116**, 017201 (2016).